IEEE Access
Multidisciplinary | Rapid Review | Open Access Journal

Received December 14, 2020, accepted January 11, 2021, date of publication January 22, 2021, date of current version February 24, 2021.

Digital Object Identifier 10.1109/ACCESS.2021.3053762

Resource Allocation for Random Selection of Distributed Jammer Towards Multistatic Radar System

XIANGTUAN WANG, TIANYAO HUANG, AND YIMIN LIU, (Member, IEEE)
Department of Electronic Engineering, Tsinghua University, Beijing 100084, China

Corresponding author: Tianyao Huang (huangtianyao@tsinghua.edu.cn)

This work was supported by the National Natural Science Foundation of China under Grant 61801258.

ABSTRACT The random array subset selection (RASS) jammer, which randomly selects a subset out of the transmit array antenna from time to time, was verified to effectively counter against multistatic radar system (MSRS). However, the countermeasure ability of RASS is restricted, because the probabilities of activating antenna elements for transmission are constrained to be identical. To further enhance the countermeasure ability, we propose the resource allocation of distributed jammer under random selection (RADJRS) in this paper, where antenna elements of the jammer are activated randomly with different probabilities, abandoning the previous constraint and generalizing RASS. We establish an optimization model with respect to the selection probabilities, whose objective function is minimizing the output-to-input jamming energy ratio of the jamming suppression method used in MSRS. This non-convex optimization model is then relaxed into a convex problem, facilitating the solution of the problem. Numerical results verify the feasibility of the relaxation and demonstrate that RADJRS outperforms the RASS when fighting against MSRS.

INDEX TERMS Random selection, resource allocation, jamming suppression, MSRS.

I. INTRODUCTION

Fighting against MSRS [1]–[3] has become an important task for the electronic countermeasure (ECM), which transmits jamming signals towards hostile radar to protect friendly target from being detected. The challenge lies in the fact that MSRS has high spatial resolution, because it synthesises large virtual antenna aperture by fusing received signals from widely separated radar systems. The enhanced angular resolution enables MSRS to distinguish the radar returns and disruptive jamming signals in spatial domain, e.g., by using some jamming suppression methods like subspace-based method [4], blind separation method [5] or adaptive filter method [6].

Utilizing jammer network to counter MSRS is a natural idea. A recent paper [7] proposed to use RASS to counter MSRS, and demonstrated that it significantly outperforms the traditional approach that applies a full antenna array to transmit jamming signals. In contrast, RASS jammer randomly selects antenna elements to transmit jamming signals, which forms stable mainlobe and random sidelobe. The random sidelobe destroys the coherence between received signals of different radar stations in MSRS, remarkably degrading the jamming suppression performance of MSRS. Following previous approach [9], it is constrained in [7] that all the array antennas are activated with the same probability. Under this constraint, it is proved that the countermeasure ability achieves its best when all the probabilities are set as $1/2$.

This paper extends the previous work [7] by omitting the equal-probability constraint, in order to further enhance the countermeasure performance against MSRS. To this end, we propose RADJRS, where the probabilities to activate antenna elements are different and are optimized under the objective of enhancing jamming performance. Therefore, RASS is a special case of RADJRS with extra constraint, and is expected to be sub-optimal to RADJRS.

Particularly, we model the optimization problem with respect to the probabilities of activating antenna elements. In the optimization model, the objective function is set to minimize the output-to-input jamming energy ratio after the jamming suppression method [8] used in MSRS, which indicates the processing gain of MSRS as well as the loss of RADJRS against MSRS.The established optimization problem is generally non-convex. To efficient solve the problem, we relax the resource allocation problem into a convex problem. Numerical results validate that such relaxation is feasible and the proposed RADJRS leads to the better countermeasure performance than the previous RASS method.

The associate editor coordinating the review of this manuscript and approving it for publication was Adnan Shahid.

The rest of this paper is organized as follows: The system and signal models of MSRS and RADJRS are introduced in Section II. Section III establishes the optimization problem with respect to probabilities of selecting antenna elements to transmit jamming signals. Simulation results are given in Section IV. Section V briefly concludes the paper.

II. SYSTEM MODEL

In this section, the geometry of the radars, jammer and target, followed by the signal models of the RADJRS is introduced. Then we analyze the advantage of the RADJRS when facing the MSRS under the adaptive filter based jamming suppression method.

A. SIGNAL MODEL OF THE JAMMER

We consider a scenario that a jammer network, closely distributed around the target, is fighting against a MSRS to protect the target from being detected. The geometry is shown in Fig. 1. The MSRS is composed of one main radar and $K-1$ auxiliary radars, which are exactly synchronized. The main radar transmits signals and receives the echoes, while the auxiliary radars operate passively, i.e., they only receive the target returns without transmitting any signals.

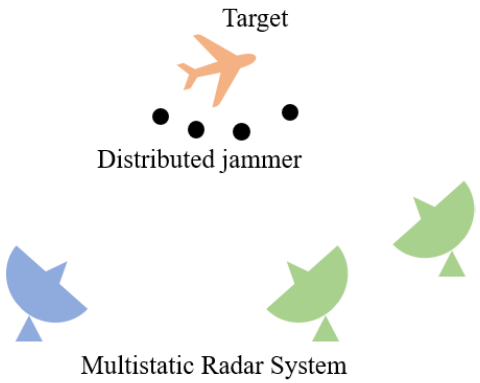

FIGURE 1. Geometry of the MSRS, target and jammer [7].

We then present the transmit signals of the jammer, which has N elements. These N elements operate coherently, which means that they are accurately synchronized and transmit the same jamming signal $r(t)$, with its autocorrelation function given by $R_{rr}(t) = \mathrm{E}[r(t)r^*(t)]$. We assume that the locations of the MSRS is known to jammer by some reconnaissance technologies or information pre-loaded by intelligence services, and the jamming signal is pointed towards the main radar. Denote by $d_{k,n}$ the distance between the n-th jammer element and the k-th radar, $k = 1, 2, \ldots, K, n = 1, 2, \ldots, N$. Here, $k = 1$ represents the main radar, and $k = 2, 3, \ldots, K$ represent the auxiliary ones. Traditional jammer operates all the elements simultaneously, and the transmit signal is given by

$$\tilde{\boldsymbol{v}}(t) = \boldsymbol{\alpha}_1\, r(t) \in \mathbb{C}^N, \tag{1}$$

where $\boldsymbol{\alpha}_k$ is the steering vector of the jammer towards the k-th radar, given by

$$\boldsymbol{\alpha}_k = \left[e^{j2\pi d_{k,1}/\lambda}, e^{j2\pi d_{k,2}/\lambda}, \ldots, e^{j2\pi d_{k,N}/\lambda}\right]^T \in \mathbb{C}^N, \tag{2}$$

and λ is the wavelength of the transmit signal.

Different from the traditional jammer, RASS jammer randomly selects a part of elements in each time slot, and the selected elements are varied from a slot to another, generating stable mainlobe and random sidelobe of the beam of jamming, as is shown in Fig. 1. To represent this, we use a random switch vector $\boldsymbol{p}(t) = [p_1(t), p_2(t), \ldots, p_N(t)]^T \in \{0, 1\}^N$ to denote which elements are operating at the time instant t. Particularly, when the n-th element is active, $p_n(t) = 1$, and 0 otherwise. The transmit signal of a RASS jammer is written as

$$\boldsymbol{v}(t) = [\boldsymbol{p}(t) \circ \boldsymbol{\alpha}_1]r(t) \in \mathbb{C}^N, \tag{3}$$

where $\circ$ is the Hadamard product. Following [7], we assume that $p_n(t)$ obeys the Bernoulli distribution with probability P_n, and $p_n(t)$ is independent with respect to the element index n and time t. The expectation of $\boldsymbol{p}(t)$ is written as

$$\boldsymbol{p}_e := \mathrm{E}[\boldsymbol{p}(t)] = [P_1, ..., P_N]^T \in \mathbb{R}^N, \tag{4}$$

and the variance of $p_n(t)$ is given by

$$\mathrm{Var}[p_n(t)] = P_n(1 - P_n). \tag{5}$$

In this paper, we abandon the assumption that $P_1 = ... = P_N$, which is used in [7]. Instead, we will study the optimization of $\boldsymbol{p}_e$ to maximize the jamming efficiency in the next section.

B. SIGNAL MODEL OF THE MSRS

We now introduce the signal model of MSRS, followed by the jamming rejection methods. The received signal $\boldsymbol{x}(t) \in \mathbb{C}^K$ is the superimposition of target echoes $\boldsymbol{s}(t) \in \mathbb{C}^K$, jamming signals $\boldsymbol{q}(t) \in \mathbb{C}^K$ and noises $\boldsymbol{n}(t) \in \mathbb{C}^K$, given by

$$\boldsymbol{x}(t) = \boldsymbol{s}(t) + \boldsymbol{q}(t) + \boldsymbol{n}(t), \tag{6}$$

where the k-th entries of these vectors, denoted by the subscript (e.g., $x_k(t)$), corresponding to the k-th radar in the MSRS. To emphasize the main radar, we let $\boldsymbol{x}_a(t) = [x_2(t), x_3(t), \ldots, x_k(t)] \in \mathbb{C}^{K-1}$ denote the signal received by the auxiliary radars. Thus, we have $\boldsymbol{x}(t) = [x_1(t), \boldsymbol{x}_a^T(t)]^T$. Similarly, we define $\boldsymbol{s}_a(t)$, $\boldsymbol{q}_a(t)$, $\boldsymbol{n}_a(t) \in \mathbb{C}^{K-1}$ such that $\boldsymbol{s}(t) = [s_1(t), \boldsymbol{s}_a^T(t)]^T$, $\boldsymbol{q}(t) = [s_1(t), \boldsymbol{q}_a^T(t)]^T$, and $\boldsymbol{n}(t) = [n_1(t), \boldsymbol{n}_a^T(t)]^T$. Here, we assume that $\boldsymbol{n}(t)$ is the white Gaussian noise with the variance of $\sigma^2\boldsymbol{I}$.

When the radar is interfered by a RASS jammer, the received jamming signal is given by

$$q_k(t) = \boldsymbol{\alpha}_k^H \boldsymbol{v}(t). \tag{7}$$

For notation convenience, we define $\boldsymbol{A} = [\boldsymbol{\alpha}_2, ..., \boldsymbol{\alpha}_K] \in \mathbb{C}^{N\times(K-1)}$, such that $\boldsymbol{q}_a(t) = \boldsymbol{A}^H\boldsymbol{v}(t)$.

We then consider the jamming suppression approach in MSRS. The main radar first estimates the jamming signal $q_1(t)$ with a linear filter, denoted by $\hat{q}_1(t) = \boldsymbol{w}^H\boldsymbol{x}_a(t)$, and

then the main radar cancel $\hat{q}_1(t)$ from the received signal to achieve jamming suppression. Here $\boldsymbol{w}$ is the filter that should be designed. We use the least mean square (LMS) adaptive filter algorithm [6] to design $\boldsymbol{w}$, given by

$$\min_{\boldsymbol{w}} \mathrm{E}\left[|q_1(t) - \boldsymbol{w}^H \boldsymbol{x}_a(t)|^2\right], \tag{8}$$

yielding $\boldsymbol{w} = \boldsymbol{r}_{1a}\boldsymbol{R}_{aa}^{-1}$, where

$$\begin{aligned} \boldsymbol{r}_{1a} &= \mathrm{E}[x_1(t)\boldsymbol{x}_a^H(t)], \\ \boldsymbol{R}_{aa} &= \mathrm{E}[\boldsymbol{x}_a(t)\boldsymbol{x}_a^H(t)]. \end{aligned} \tag{9}$$

The estimate of $q_1(t)$ is then expressed as

$$\hat{q}_1(t) = \boldsymbol{r}_{1a}\boldsymbol{R}_{aa}^{-1}\boldsymbol{x}_a(t). \tag{10}$$

For the sampling signal with points number L, the above matrices can be obtained as the sampled correlation matrices by

$$\begin{aligned} \hat{\boldsymbol{r}}_{1a} &= \sum_{t=1}^{L} x_1(t)\boldsymbol{x}_a^H(t), \\ \hat{\boldsymbol{R}}_{aa} &= \sum_{t=1}^{L} \boldsymbol{x}_a(t)\boldsymbol{x}_a^H(t). \end{aligned} \tag{11}$$

Then, the estimation of jamming signal is eliminated from the main radar, given by

$$x_1(t) - \hat{q}_1(t) = s_1(t) + n_1(t) + q_1(t) - \hat{q}_1(t). \tag{12}$$

Here, $q_1(t) - \hat{q}_1(t)$ is the remainder of the jamming signal after jamming suppression method.

In the next section, we will optimize $\boldsymbol{p}_e$ to increase the remainder energy of the jamming signals.

III. TRANSMIT PROBABILITIES OPTIMIZATION

In this section, we aim at maximizing the jamming performance by optimizing the transmit probabilities $\boldsymbol{p}_e$. Particularly, we use the output-to-input jamming energy ratio to evaluate the jamming performance (which will be explained later), and model an optimization problem that maximizes this ratio. To solve the optimization problem efficiently, we relax it into a convex problem.

A. OPTIMIZATION CRITERION

We use the output-to-input jamming energy ratio to evaluate the performance of the jamming suppression method, given by

$$\beta = J_o/J_i, \tag{13}$$

where $J_o = \mathrm{E}[|q_1(t) - \hat{q}_1(t)|^2]$ and $J_i = \mathrm{E}[q_1(t)q_1^*(t)]$ are the output and input energy of the jamming signals under the jamming elimination method, respectively. In a jamming scenario, radar performance mainly relies on the remained energy of jamming signals. Therefore, we adopt the output-to-input jamming energy ratio as criterion rather than evaluating the signal intensity received by the radar. Particularly, β indicates the jamming suppression performance of radar: For an effective suppression method, J_o is expected to be far less than J_i, which leads to a small value of β. Therefore, higher values of the ratio β indicate worse performance of the jamming suppression method. We note that both J_o and J_i rely on the values of $\boldsymbol{p}_e$.

We aim at affecting the jamming rejection performance of MSRS, by carefully designing $\boldsymbol{p}_e$. We regard this as a resource allocation problem, because the probability P_n, the n-th entry of $\boldsymbol{p}_e$, represents the availability of the n-th element, a kind of hardware resource allocated for jamming. Particularly, we model the following constrained optimization problem:

$$\max_{\boldsymbol{p}_e} \frac{J_o}{J_i}, \quad \text{s.t. } 0 \le P_n \le 1,\ n = 1, ..., N. \tag{14}$$

By substituting the expressions of J_o, J_i and $\hat{q}_1(t)$ in (10) into (13), we rewrite (13) as

$$\beta = \sigma^2 \frac{\boldsymbol{\alpha}_1^H \boldsymbol{U}(\boldsymbol{U}^H\boldsymbol{A}\boldsymbol{A}^H\boldsymbol{U} + \sigma^2\boldsymbol{I})^{-1}\boldsymbol{U}^H\boldsymbol{\alpha}_1}{\boldsymbol{\alpha}_1^H\boldsymbol{U}\boldsymbol{U}^H\boldsymbol{\alpha}_1}, \tag{15}$$

where $\boldsymbol{U} \in \mathbb{C}^{N\times N}$ is a matrix satisfying

$$\boldsymbol{U}\boldsymbol{U}^H = \boldsymbol{V} := \mathrm{E}[\boldsymbol{v}(t)\boldsymbol{v}^H(t)], \tag{16}$$

and depends on $\boldsymbol{p}_e$. We put the proof of (15) in the Appendix A for the sake of readability.

The objective function (15) with respect to $\boldsymbol{p}_e$ is quite complex. In the sequel, we will first simply the optimization problem by relaxing the objective function.

B. RELAXED OBJECTIVE FUNCTION

Observing (15), we let $\tilde{\boldsymbol{\alpha}} = \boldsymbol{U}^H\boldsymbol{\alpha}_1$, and then β has a form of Rayleigh quotient with respect to $\boldsymbol{B}^{-1}$, i.e.,

$$\beta = \sigma^2 \frac{\tilde{\boldsymbol{\alpha}}^H\boldsymbol{B}^{-1}\tilde{\boldsymbol{\alpha}}}{\tilde{\boldsymbol{\alpha}}^H\tilde{\boldsymbol{\alpha}}}, \tag{17}$$

where $\boldsymbol{B} = \boldsymbol{U}^H\boldsymbol{A}\boldsymbol{A}^H\boldsymbol{U} + \sigma^2\boldsymbol{I}$. According to [10], the β is bounded by the eigenvalues of $\boldsymbol{B}^{-1}$, i.e.

$$\lambda_{\min}(\boldsymbol{B}^{-1}) \le \beta \le \lambda_{\max}(\boldsymbol{B}^{-1}), \tag{18}$$

where $\lambda_{\min}(\cdot)$ and $\lambda_{\max}(\cdot)$ represent the minimum and maximum eigenvalues of a matrix, respectively. By the property of eigenvalue of inverse matrix, we have the following inequalities,

$$\frac{1}{\lambda_{\max}(\boldsymbol{B})} \le \beta \le \frac{1}{\lambda_{\min}(\boldsymbol{B})}. \tag{19}$$

Instead of directly maximizing β, we minimize $\lambda_{\max}(\boldsymbol{B})$. Since the eigenvalues of $\boldsymbol{U}^H\boldsymbol{A}\boldsymbol{A}^H\boldsymbol{U} + \sigma^2\boldsymbol{I}$ equal to those of $\boldsymbol{A}^H\boldsymbol{V}\boldsymbol{A} + \sigma^2\boldsymbol{I}$, respectively [10], we relax the optimization problem (14) to

$$\begin{aligned} &\min_{\boldsymbol{p}_e} \lambda_{\max}\left(\boldsymbol{A}^H\boldsymbol{V}\boldsymbol{A} + \sigma^2\boldsymbol{I}\right), \\ &\text{s.t. } 0 \le P_n \le 1, \quad n = 1, ..., N. \end{aligned} \tag{20}$$

Since (20) is a convex problem, as stated in the following proposition, global optimal solution can be obtained with some generic convex toolboxes. The (20) can be transformed

in to a semi-definite programming problem (SDP). With a certain solution accuracy ϵ, in the worst case the complexity of the SDP problem solved by primal-dual interior-point algorithm is $\mathcal{O}(N^{4.5}\log(1/\epsilon))$.

Proposition 1: The optimization problem (20) *is equivalent with a convex problem.*

Proof: See Appendix B for the proof and a brief discussion on the computational complexity. □

Particularly, when we impose the assumption $P_1 = ... = P_N$ to (20), implying the resource allocation problem in [7], we obtain the solution $P_1 = ... = P_N = 0.5$ as present in the following proposition.

Proposition 2: The objective of the following optimization problem

$$\begin{aligned} &\min_{\boldsymbol{p}_e} \ \lambda_{\max}\left(\boldsymbol{A}^H\boldsymbol{V}\boldsymbol{A}+\sigma^2\boldsymbol{I}\right), \\ &\text{s.t. } 0 \le P_n \le 1, \quad n = 1, ..., N, \\ &\qquad P_1 = P_2 = \cdots = P_N. \end{aligned} \tag{21}$$

reaches its minimum when $P_1 = ... = P_N = 0.5$.

Proof: See Appendix C. □

Since (21) is a special case of (20), (20) yields better countermeasure ability. In the next section, numerical results are given to validate our analysis.

IV. NUMERICAL RESULTS

In this section, the performance of the proposed optimized RADJRS is demonstrated by numerical results. First, we give the simulation settings. Next, we compare the original objective function in (14) with its relaxation in (20). Finally, we show numerical results of jamming performance, which indicate that the proposed RADJRS outperforms the traditional RASS.

We consider an MSRS with $K = 6$ radars. Their three dimensional coordinates are set as follows: (0,0,0) m, (200,0,0) m, (0,200,0) m, (200,200,0) m, (300,0,0) m and (0,300,0) m. The target is located at (2,2,15) km, equipped with a jammer closely positioned to it. The array elements of the jammer share the same x and y coordinates with the target, while their z coordinates are set randomly. The first radar is the main radar, transmitting linear frequency modulation (LFM) signal with the bandwidth of 10 MHz, the duration of 10 μs and the center frequency of 5 GHz. We uniformly divide the duration of LFM into $L = 200$ time slots. The $\sigma^2 = 10^{-2}$ is the radar receive noise variance and the $\frac{\mathrm{E}[||q_1(t)||_2^2]}{\mathrm{E}[||n_1(t)||_2^2]} = 40$ dB. The jammer uses Gaussian noise of the same bandwidth as its baseband signal $r(t)$, continuously jamming towards the main radar. The input JSR with respect to each element of jammer's array antenna is set as $\frac{\mathrm{E}[||q_1(t)||_2^2]}{\mathrm{E}[||s_1(t)||_2^2]} = 23$ dB. The distributed jammer randomly transmit jamming signal in each time slot.

In the first experiment, we consider the relationship between the output-to-input jamming energy ratio β and the relaxed one $\lambda_{\max}\left(\boldsymbol{A}^H\boldsymbol{V}\boldsymbol{A}+\sigma^2\boldsymbol{I}\right)$. In this experiment, we perform 10000 Monte-Carlo trials. In each trial, we randomly generate $\boldsymbol{p}_e$, and then calculate the corresponding β and $\lambda_{\max}\left(\boldsymbol{A}^H\boldsymbol{V}\boldsymbol{A}+\sigma^2\boldsymbol{I}\right)$, yielding a pair $(\beta, \lambda_{\max}\left(\boldsymbol{A}^H\boldsymbol{V}\boldsymbol{A}+\sigma^2\boldsymbol{I}\right))$. All the pairs are shown together in Fig. 2, from which we find that when the β achieves its maximum, the corresponding $\lambda_{\max}\left(\boldsymbol{A}^H\boldsymbol{V}\boldsymbol{A}+\sigma^2\boldsymbol{I}\right)$ achieves its minimum. Therefore, it is feasible to use (20) as a relaxation of the original resource allocation problem (14).

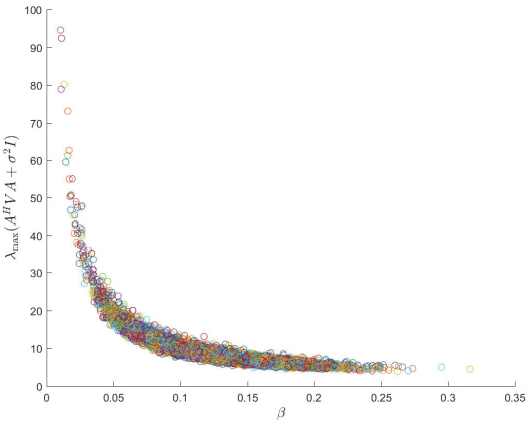

FIGURE 2. The relationship between β and $\lambda_{\max}\left(A^HVA+\sigma^2I\right)$.

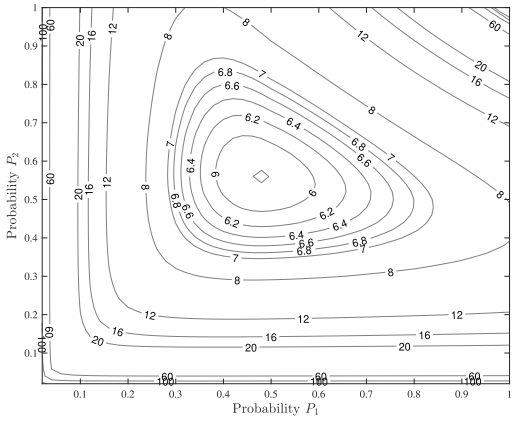

FIGURE 3. Values of $\lambda_{\max}\left(A^HVA+\sigma^2I\right)$ versus $p_e = [P_1, P_2]^T$.

Next, we depict the shape of objective function $\lambda_{\max}\left(\boldsymbol{A}^H\boldsymbol{V}\boldsymbol{A}+\sigma^2\boldsymbol{I}\right)$ versus the jamming transmit probability $\boldsymbol{p}_e$. In this experiment, the jammer has $N = 2$ elements with the z coordinates being 15006 m and 15116 m. The transmit probability P_1 and P_2 range from 0.02 to 1 with a step of 0.02, and $\lambda_{\max}\left(\boldsymbol{A}^H\boldsymbol{V}\boldsymbol{A}+\sigma^2\boldsymbol{I}\right)$ is calculated at each grid of (P_1, P_2). The results is shown in Fig. 3. From this figure, we find that the objective function is convex, verifying Proposition 1. Larger value of $\lambda_{\max}\left(\boldsymbol{A}^H\boldsymbol{V}\boldsymbol{A}+\sigma^2\boldsymbol{I}\right)$ represents lower value of β and thus worse jamming performance. We also find that four corners of the figure have large values of $\lambda_{\max}\left(\boldsymbol{A}^H\boldsymbol{V}\boldsymbol{A}+\sigma^2\boldsymbol{I}\right)$. For example, at the upper right corner of figure (where $P_1 = P_2 = 1$), which means that the elements are transmitting jamming signal deterministically all the time, $\lambda_{\max}\left(\boldsymbol{A}^H\boldsymbol{V}\boldsymbol{A}+\sigma^2\boldsymbol{I}\right)$ reaches its maximum.

This phenomenon indicates that the randomness on selecting transmit elements is important to fight against MSRS.

In addition, we compare the global minimum and the minimum along the anti-diagonal of Fig. 3. The former represents the optimal performance that the proposed RADJRS can achieve, while the latter is the optimum that the previous RASS method [7] reaches, because the anti-diagonal expresses the constraint of $P_1 = P_2$. The global minimum is 5.712, achieved at (0.46, 0.54), lower than the minimum along the anti-diagonal, 5.9067, achieved when $P_1 = P_2 = 0.5$. The result indicates the necessity of omitting the constraint $P_1 = P_2$ and optimizing the entries of $\boldsymbol{p}_e$.

Finally, we compare the performance of RASS and RADJRS under the constraint of fixed transmit energy $\|\boldsymbol{p}_e\|_2$. We set $\|\boldsymbol{p}_e\|_2 = \sqrt{N}p$, and we vary p from 0.1 to 1 with step 0.1. In RASS, the jamming transmit probability $\boldsymbol{p}_{e1}$ follows $P_1 = ... = P_N = p$. In RADJRS, the transmit probability $\boldsymbol{p}_e$ is obtained by solving (20) with an additional constraint $\|\boldsymbol{p}_e\|_2 = \sqrt{N}p$ (which is still convex). We set $N = 3$, and the z coordinates of jammer's array elements are 15006 m, 15116 m and 15188 m, respectively. The results are presented in Fig. 4, where each dot of RASS is obtained by 100 Monte Carlo trials. The results are simulated under a computer with an Intel 3.30 GHz i5-4590 CPU and 8GB RAM. The dots of RADJRS are obtained with convex toolbox, where the CPU computing times range from 0.53s to 0.69s. By applying more efficient convex solvers or some greedy approaches, we may further reduce the consuming time, to meet real-time computation requirements. We remain this for future investigation. As is shown in Fig. 4, RADJRS achieves higher β than RASS, indicating the advantage of RADJRS over RASS.

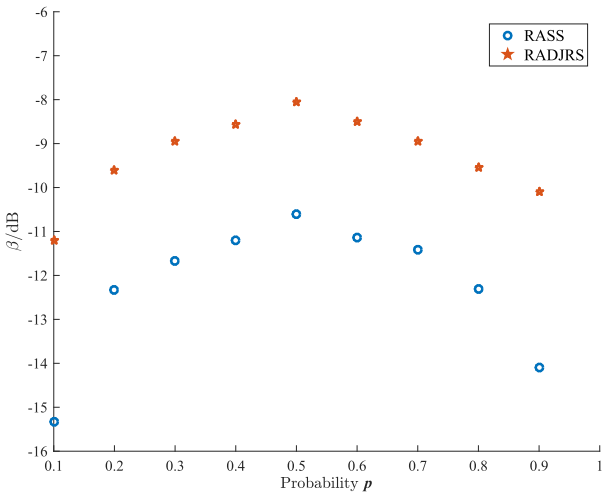

FIGURE 4. The output-to-input jamming energy ratio β of RASS and RADJRS versus p under the average energy constraint $\|p_e\|_2 = \sqrt{N}p$.

V. CONCLUSION

In this paper, the RADJRS, whose array elements use different probabilities to transmit jamming signal, was proposed to enhance countermeasure ability of jammer. The transmit probabilities of array elements are optimized by maximizing the output-to-input jamming energy ratio of radar, which uses LMS adaptive filter to suppress jamming signal. To solve the optimization problem efficiently, we relax it into a convex problem. Simulation results demonstrate that the proposed method significantly improves the jamming performance and energy transmit efficiency over the previous RASS method that restricts the transmit probabilities of jamming elements being identical.

.

APPENDIX A
PROOF OF (15)

In this appendix, we provide the proof of (15). We will provides the deductions of the numerator and denominator in (13) to give the proof. Firstly, we provide the expressions of numerator and denominator under our signal model. Then the eigen-decomposition method is used to simplify the numerator to achieve (13).

In (13), the numerator is written as $J_o = \mathrm{E}[|q_1(t) - \hat{q}_1(t)|^2]$ and the denominator is written as $J_i = \mathrm{E}[q_1(t)q_1^*(t)]$.

Firstly, we provide the deduction of the numerator J_o. The $J_o = \mathrm{E}[|q_1(t) - \hat{q}_1(t)|^2]$ can be further expressed as

$$\begin{aligned}\mathrm{E}[|q_1(t) - \hat{q}_1(t)|^2] = \mathrm{E}[q_1(t)q_1^*(t)] + \mathrm{E}[\hat{q}_1(t)\hat{q}_1^*(t)] \\ - \mathrm{E}[q_1(t)\hat{q}_1^*(t)] - \mathrm{E}[\hat{q}_1(t)q_1^*(t)].\end{aligned} \tag{22}$$

There are four expectations in the right side of the (22). The expressions of $q_1(t)$ and $\hat{q}_1(t)$ is given in (7) and (10) respectively. Then we can provide the expressions of the expectations as following:

$$\begin{aligned}\mathrm{E}[q_1(t)q_1^*(t)] &= \mathrm{E}[\boldsymbol{\alpha}_1^H \boldsymbol{v}(t)\boldsymbol{v}^H(t)\boldsymbol{\alpha}_1] \\ &= \boldsymbol{\alpha}_1^H \mathrm{E}[\boldsymbol{v}(t)\boldsymbol{v}^H(t)]\boldsymbol{\alpha}_1 \\ &= \boldsymbol{\alpha}_1^H \boldsymbol{V}\boldsymbol{\alpha}_1, \end{aligned} \tag{23}$$

$$\begin{aligned}\mathrm{E}[\hat{q}_1(t)\hat{q}_1^*(t)] &= \mathrm{E}[\boldsymbol{r}_{1a}\boldsymbol{R}_{aa}^{-1}\boldsymbol{x}_a(t)\boldsymbol{x}_a^H(t)\boldsymbol{R}_{aa}^{-H}\boldsymbol{r}_{1a}] \\ &= \boldsymbol{r}_{1a}\boldsymbol{R}_{aa}^{-1}\mathrm{E}[\boldsymbol{x}_a(t)\boldsymbol{x}_a^H(t)]\boldsymbol{R}_{aa}^{-H}\boldsymbol{r}_{1a}^H \\ &= \boldsymbol{r}_{1a}\boldsymbol{R}_{aa}^{-1}\boldsymbol{R}_{aa}\boldsymbol{R}_{aa}^{-H}\boldsymbol{r}_{1a}^H \\ &= \boldsymbol{r}_{1a}\boldsymbol{R}_{aa}^{-H}\boldsymbol{r}_{1a}^H, \end{aligned} \tag{24}$$

$$\begin{aligned}\mathrm{E}[q_1(t)\hat{q}_1^*(t)] &= \mathrm{E}[\boldsymbol{\alpha}_1^H \boldsymbol{v}(t)\boldsymbol{x}_a^H(t)\boldsymbol{R}_{aa}^{-H}\boldsymbol{r}_{1a}^H] \\ &= \boldsymbol{\alpha}_1^H \mathrm{E}[\boldsymbol{v}(t)\boldsymbol{q}_a^H(t)]\boldsymbol{R}_{aa}^{-H}\boldsymbol{r}_{1a}^H \\ &= \boldsymbol{\alpha}_1^H \mathrm{E}[\boldsymbol{v}(t)\boldsymbol{v}^H(t)\boldsymbol{A}]\boldsymbol{R}_{aa}^{-H}\boldsymbol{r}_{1a}^H \\ &= \boldsymbol{\alpha}_1^H \boldsymbol{V}\boldsymbol{A}\boldsymbol{R}_{aa}^{-H}\boldsymbol{r}_{1a}^H \end{aligned} \tag{25}$$

and

$$\begin{aligned}\mathrm{E}[\hat{q}_1(t)q_1^*(t)] &= \mathrm{E}[\boldsymbol{r}_{1a}\boldsymbol{R}_{aa}^{-1}\boldsymbol{x}_a(t)\boldsymbol{v}^H(t)\boldsymbol{\alpha}_1] \\ &= \boldsymbol{r}_{1a}\boldsymbol{R}_{aa}^{-1}\mathrm{E}[\boldsymbol{q}_a(t)\boldsymbol{v}^H(t)]\boldsymbol{\alpha}_1 \\ &= \boldsymbol{r}_{1a}\boldsymbol{R}_{aa}^{-1}\mathrm{E}[\boldsymbol{A}^H\boldsymbol{v}(t)\boldsymbol{v}^H(t)]\boldsymbol{\alpha}_1 \\ &= \boldsymbol{r}_{1a}\boldsymbol{R}_{aa}^{-1}\boldsymbol{A}^H\boldsymbol{V}\boldsymbol{\alpha}_1. \end{aligned} \tag{26}$$

The above deductions use the assumption that the target echoes, jamming and noise are mutually uncorrelated, e.g. $\mathrm{E}[\boldsymbol{q}_a(t)\boldsymbol{s}_a^H(t)] = 0$, $\mathrm{E}[\boldsymbol{q}_a(t)\boldsymbol{n}_a^H(t)] = 0$ and $\mathrm{E}[\boldsymbol{s}_a(t)\boldsymbol{n}_a^H(t)] = 0$.

The $\boldsymbol{r}_{1a}$ and $\boldsymbol{R}_{aa}$ are the cross-correlation and autocorrelation as given in (9).

$$\begin{aligned}\boldsymbol{r}_{1a} &= \mathrm{E}[x_1(t)\boldsymbol{x}_a^H(t)]\\ &= \mathrm{E}[(s_1(t)+q_1(t)+n_1(t))(\boldsymbol{s}_a(t)+\boldsymbol{q}_a(t)+\boldsymbol{n}_a(t))^H]\\ &= \mathrm{E}[q_1(t)\boldsymbol{q}_a^H(t)]\\ &= \mathrm{E}[\boldsymbol{\alpha}_1^H\boldsymbol{v}(t)\boldsymbol{v}^H(t)\boldsymbol{A}]\\ &= \boldsymbol{\alpha}_1^H\boldsymbol{V}\boldsymbol{A} \end{aligned} \tag{27}$$

and

$$\begin{aligned}\boldsymbol{R}_{aa} &= \mathrm{E}[\boldsymbol{x}_a(t)\boldsymbol{x}_a^H(t)]\\ &= \mathrm{E}[(\boldsymbol{s}_a(t)+\boldsymbol{q}_a(t)+\boldsymbol{n}_a(t))(\boldsymbol{s}_a(t)+\boldsymbol{q}_a(t)+\boldsymbol{n}_a(t))^H]\\ &= \sigma^2\boldsymbol{I}+\mathrm{E}[\boldsymbol{q}_a(t)\boldsymbol{q}_a^H(t)]\\ &= \sigma^2\boldsymbol{I}+\boldsymbol{A}^H\boldsymbol{V}\boldsymbol{A}. \end{aligned} \tag{28}$$

Then we take the expression of $\boldsymbol{r}_{1a}$ and $\boldsymbol{R}_{aa}$ into the four expectations,

$$\begin{aligned}&\mathrm{E}[q_1(t)q_1^*(t)] = \boldsymbol{\alpha}_1^H\boldsymbol{V}\boldsymbol{\alpha}_1,\\ &\mathrm{E}[\hat{q}_1(t)\hat{q}_1^*(t)] = \boldsymbol{\alpha}_1^H\boldsymbol{V}\boldsymbol{A}(\sigma^2\boldsymbol{I}+\boldsymbol{A}^H\boldsymbol{V}\,\boldsymbol{A})^{-H}\boldsymbol{A}^H\boldsymbol{V}\boldsymbol{\alpha}_1,\\ &\mathrm{E}[q_1(t)\hat{q}_1^*(t)] = \boldsymbol{\alpha}_1^H\boldsymbol{V}\,\boldsymbol{A}(\sigma^2\boldsymbol{I}+\boldsymbol{A}^H\boldsymbol{V}\,\boldsymbol{A})^{-H}\boldsymbol{A}^H\boldsymbol{V}\boldsymbol{\alpha}_1,\\ &\mathrm{E}[\hat{q}_1(t)q_1^*(t)] = \boldsymbol{\alpha}_1^H\boldsymbol{V}\boldsymbol{A}(\sigma^2\boldsymbol{I}+\boldsymbol{A}^H\boldsymbol{V}\boldsymbol{A})^{-1}\boldsymbol{A}^H\boldsymbol{V}\boldsymbol{\alpha}_1. \end{aligned} \tag{29}$$

Taking the (29) into the (22), we can get the expression of J_o in our signal model, written as

$$\begin{aligned}&\mathrm{E}[|q_1(t)-\hat{q}_1(t)|^2]\\ &\quad= \boldsymbol{\alpha}_1^H\boldsymbol{V}\boldsymbol{\alpha}_1-\boldsymbol{\alpha}_1^H\boldsymbol{V}\boldsymbol{A}(\sigma^2\boldsymbol{I}+\boldsymbol{A}^H\boldsymbol{V}\boldsymbol{A})^{-1}\boldsymbol{A}^H\boldsymbol{V}\boldsymbol{\alpha}_1. \end{aligned} \tag{30}$$

Next, we will use the eigen-decomposition method to simply the J_o in (30).

According to (16), the $\boldsymbol{V}$ can be expressed as $\boldsymbol{V} := \boldsymbol{U}\boldsymbol{U}^H$. Then the (22) can be derived into

$$\begin{aligned}&\mathrm{E}[|q_1(t)-\hat{q}_1(t)|^2]\\ &\quad= \boldsymbol{\alpha}_1^H\boldsymbol{U}[\boldsymbol{I}-\boldsymbol{U}^H\boldsymbol{A}(\sigma^2\boldsymbol{I}+\boldsymbol{A}^H\boldsymbol{U}\boldsymbol{U}^H\boldsymbol{A})^{-1}\boldsymbol{A}^H\boldsymbol{U}]\boldsymbol{U}^H\boldsymbol{\alpha}_1. \end{aligned} \tag{31}$$

We define $\boldsymbol{B}$ with $\boldsymbol{B} := \boldsymbol{A}^H\boldsymbol{U}$, and the singular decomposition of $\boldsymbol{B}$ is written as $\boldsymbol{B} := \boldsymbol{\Psi}\boldsymbol{\Sigma}\boldsymbol{\Gamma}^H$. Then expression in the square brackets in (31) can be deducted into

$$\begin{aligned}&\boldsymbol{I}-\boldsymbol{U}^H\boldsymbol{A}(\sigma^2\boldsymbol{I}+\boldsymbol{A}^H\boldsymbol{U}\boldsymbol{U}^H\boldsymbol{A})^{-1}\boldsymbol{A}^H\boldsymbol{U}\\ &\quad= \boldsymbol{I}-\boldsymbol{B}^H(\sigma^2\boldsymbol{I}+\boldsymbol{B}\boldsymbol{B}^H)^{-1}\boldsymbol{B}\\ &\quad= \boldsymbol{I}-\boldsymbol{\Gamma}\boldsymbol{\Sigma}^H\boldsymbol{\Psi}^H(\sigma^2\boldsymbol{I}+\boldsymbol{\Psi}\boldsymbol{\Sigma}\boldsymbol{\Gamma}^H\boldsymbol{\Gamma}\boldsymbol{\Sigma}^H\boldsymbol{\Psi}^H)^{-1}\boldsymbol{\Psi}\boldsymbol{\Sigma}\boldsymbol{\Gamma}^H\\ &\quad= \boldsymbol{I}-\boldsymbol{\Gamma}\boldsymbol{\Sigma}^H\boldsymbol{\Psi}^H[\boldsymbol{\Psi}(\boldsymbol{\Sigma}\boldsymbol{\Sigma}^H+\sigma^2\boldsymbol{I})\boldsymbol{\Psi}^H]^{-1}\boldsymbol{\Psi}\boldsymbol{\Sigma}\boldsymbol{\Gamma}^H\\ &\quad= \boldsymbol{I}-\boldsymbol{\Gamma}\boldsymbol{\Sigma}^H\boldsymbol{\Psi}^H\boldsymbol{\Psi}(\boldsymbol{\Sigma}\boldsymbol{\Sigma}^H+\sigma^2\boldsymbol{I})^{-1}\boldsymbol{\Psi}^H\boldsymbol{\Psi}\boldsymbol{\Sigma}\boldsymbol{\Gamma}^H\\ &\quad= \boldsymbol{I}-\boldsymbol{\Gamma}\boldsymbol{\Sigma}^H(\boldsymbol{\Sigma}\boldsymbol{\Sigma}^H+\sigma^2\boldsymbol{I})^{-1}\boldsymbol{\Sigma}\boldsymbol{\Gamma}^H\\ &\quad= \sigma^2\boldsymbol{\Gamma}(\boldsymbol{\Sigma}\boldsymbol{\Sigma}^H+\sigma^2\boldsymbol{I})^{-1}\boldsymbol{\Gamma}^H\\ &\quad= \sigma^2(\sigma^2\boldsymbol{I}+\boldsymbol{U}^H\boldsymbol{A}\boldsymbol{A}^H\boldsymbol{U})^{-1}. \end{aligned} \tag{32}$$

Then the(22) can be simplified as

$$\mathrm{E}[|q_1(t)-\hat{q}_1(t)|_2^2] = \sigma^2\boldsymbol{\alpha}_1^H\boldsymbol{U}(\sigma^2\boldsymbol{I}+\boldsymbol{U}^H\boldsymbol{A}\boldsymbol{A}^H\boldsymbol{U})^{-1}\boldsymbol{U}^H\boldsymbol{\alpha}_1, \tag{33}$$

which is the numerator given in (15).

Next we consider the denominator $J_i = \mathrm{E}[q_1(t)q_1^H(t)]$, whose expression is given in (23). Then we have $J_i = \boldsymbol{\alpha}_1^H\boldsymbol{V}\boldsymbol{\alpha}_1$, which is the denominator in (15). Then we can get the (15).

APPENDIX B
PROOF OF PROPOSITION 1

In this appendix, we provide the proof of Proposition 1. Firstly, we transform the objective function into a semi-definite programming problem with a linear objective function and a inequality constraints. Then we use the definition of quasiconvex function to show that the inequality constraints is quasiconvex. By [11], the quasiconvex constraints is equivalent to a class of convex constraints. Then we can proof that the (20) is equivalent to a convex problem.

Firstly, we transform the eigenvalue objective function under semi-definite programming (SDP). The (20) is transformed into [11]

$$\begin{aligned}&\min_{\boldsymbol{p}_e,\,\gamma}\ \gamma\\ &\text{s.t. } \gamma\boldsymbol{I}-\sigma^2\boldsymbol{I}-\boldsymbol{A}^H\boldsymbol{V}(\boldsymbol{p}_e)\boldsymbol{A}\preceq 0,\\ &\quad \boldsymbol{0}\le\boldsymbol{p}_e\le\boldsymbol{1}. \end{aligned} \tag{34}$$

In the (34), the objective function γ and the constraint $\boldsymbol{0}\le\boldsymbol{p}_e\le\boldsymbol{1}$ are linear. So we should analyze the convexity of the first constraints. Then we will consider the convexity of the function $\boldsymbol{V}(\boldsymbol{p}_e)$.

To analysis the convexity of the constraints, we firstly provide the expression of $\boldsymbol{V}$. According to (16), the $\boldsymbol{V}$ is the expectation written as

$$\begin{aligned}\boldsymbol{V} :&= \mathrm{E}[\boldsymbol{v}(t)\boldsymbol{v}^H(t)]\\ &= \mathrm{E}[\boldsymbol{p}(t)\circ\boldsymbol{\alpha}_1(\boldsymbol{p}(t)\circ\boldsymbol{\alpha}_1)^H]\mathrm{E}[r(t)r^*(t)]\\ &= \mathrm{E}[(\boldsymbol{p}(t)\circ\boldsymbol{\alpha}_1)(\boldsymbol{p}(t)\circ\boldsymbol{\alpha}_1)^H]R_{rr}(t) \end{aligned} \tag{35}$$

We firstly give the expression of $\boldsymbol{p}(t)\circ\boldsymbol{\alpha}_1$ and $(\boldsymbol{p}(t)\circ\boldsymbol{\alpha}_1)(\boldsymbol{p}(t)\circ\boldsymbol{\alpha}_1)^H$ as following

$$\begin{aligned}&\boldsymbol{p}(t)\circ\boldsymbol{\alpha}_1\\ &\quad= \begin{pmatrix} p_1(t)\alpha_{11}\\ \vdots\\ p_N(t)\alpha_{1N}\end{pmatrix},\\ &(\boldsymbol{p}(t)\circ\boldsymbol{\alpha}_1)(\boldsymbol{p}(t)\circ\boldsymbol{\alpha}_1)^H\\ &\quad= \begin{pmatrix} p_1^2(t)\alpha_{11}\alpha_{11}^* & \cdots & p_1(t)p_N(t)\alpha_{11}\alpha_{1N}^*\\ \vdots & \ddots & \vdots\\ p_1(t)p_N(t)\alpha_{1N}\alpha_{11}^* & \cdots & p_N^2(t)\alpha_{1N}\alpha_{1N}^*\end{pmatrix}. \end{aligned} \tag{36}$$

By the assumption that $\mathrm{E}[p_n^2(t)] = P_n, \mathrm{E}[p_n(t)p_m(t)] = P_nP_m$ and $\alpha_{1n}\alpha_{1n}^* = 1$, we can get the expression of $\mathrm{E}[(\boldsymbol{p}(t)\circ$

$\boldsymbol{\alpha}_1)(\boldsymbol{p}(t)\circ\boldsymbol{\alpha}_1)^H]$ as

$$\begin{aligned}&\mathrm{E}[(\boldsymbol{p}(t)\circ\boldsymbol{\alpha}_1)(\boldsymbol{p}(t)\circ\boldsymbol{\alpha}_1)^H]\\&=\begin{pmatrix}P_1 & \dots & P_1P_N\alpha_{11}\alpha_{1N}^*\\ \vdots & \ddots & \vdots\\ P_1P_N\alpha_{1N}\alpha_{11}^* & \dots & P_N\end{pmatrix}\\&=(\boldsymbol{p}_e\circ\boldsymbol{\alpha}_1)(\boldsymbol{p}_e\circ\boldsymbol{\alpha}_1)^H+\mathrm{diag}[\boldsymbol{p}_e\circ(\boldsymbol{1}-\boldsymbol{p}_e)].\end{aligned}\tag{37}$$

Then the $\boldsymbol{V}(\boldsymbol{p}_e)$ is expressed as

$$\boldsymbol{V}=\{(\boldsymbol{p}_e\circ\boldsymbol{\alpha}_1)(\boldsymbol{p}_e\circ\boldsymbol{\alpha}_1)^H+\mathrm{diag}[\boldsymbol{p}_e\circ(\boldsymbol{1}-\boldsymbol{p}_e)]\}R_{rr}(t).\tag{38}$$

Let $\boldsymbol{P}\in\mathbb{C}^{N\times N}:=\mathrm{diag}(\boldsymbol{p}_e)$, the $\boldsymbol{V}$ can be written as

$$\boldsymbol{V}(\boldsymbol{P})=[\boldsymbol{P}\boldsymbol{\alpha}_1\boldsymbol{\alpha}_1^H\boldsymbol{P}+\boldsymbol{P}(\boldsymbol{I}-\boldsymbol{P})]R_{rr}(t).\tag{39}$$

Here we definite $\boldsymbol{\Phi}:=\boldsymbol{\alpha}_1\boldsymbol{\alpha}_1^H$. Then $\boldsymbol{V}(\boldsymbol{P})=[\boldsymbol{P}\boldsymbol{\Phi}\boldsymbol{P}+\boldsymbol{P}(\boldsymbol{I}-\boldsymbol{P})]R_{rr}(t)$.

We use the following definition to analyze the convexity of $\boldsymbol{V}(\boldsymbol{P})$ [11]: A function is convex (or quasiconvex) if and only if it is convex (or quasiconvex) on any line which intersects the domain of the function.

Then we consider an arbitrary line located in the domain of $\boldsymbol{V}(\boldsymbol{P})$, i.e $\boldsymbol{V}(\boldsymbol{P}+y\Delta\boldsymbol{P})$. Let $g(y)=\boldsymbol{V}(\boldsymbol{P}+y\Delta\boldsymbol{P})/R_{rr}(t)$. Then we use the first order and second order derivatives of $g(y)$ to judge the convexity of $g(y)$. The expression of derivatives of $g(y)$ is written as

$$g(y)=(\boldsymbol{P}+y\Delta\boldsymbol{P})\boldsymbol{\Phi}(\boldsymbol{P}+y\Delta\boldsymbol{P})+(\boldsymbol{P}+y\Delta\boldsymbol{P})[\boldsymbol{I}-(\boldsymbol{P}+y\Delta\boldsymbol{P})].\tag{40}$$

Then we calculate the first order and second order derivatives of $g(y)$, written as follows:

$$\frac{\partial g}{\partial y}=\Delta\boldsymbol{P}+2\Delta\boldsymbol{P}(\boldsymbol{\Phi}-\boldsymbol{I})(\boldsymbol{P}+y\Delta\boldsymbol{P}),\tag{41}$$

$$\frac{\partial^2 g}{\partial y^2}=2\Delta\boldsymbol{P}(\boldsymbol{\Phi}-\boldsymbol{I})\Delta\boldsymbol{P}.\tag{42}$$

We firstly analysis the second order derivative. In (42), the $\Delta\boldsymbol{P}$ are non-negative diagonal matrix, the $\boldsymbol{\Phi}=\boldsymbol{\alpha}_1\boldsymbol{\alpha}_1^H$ is a rank-1 matrix. Thus the $\boldsymbol{\Phi}-\boldsymbol{I}$ has one non-negative eigenvalue and $K-1$ negative eigenvalues. The second order derivative is not positive definite or negative definite. So the $g(y)$ is not convex or concave.

Next, we will proof that the $g(y)$ is a quasiconcave function. We present the proof by a necessary and sufficient condition of quasiconcave function [11], i.e. $\frac{\partial g}{\partial y}=0\implies\frac{\partial^2 g}{\partial y^2}\le 0$.

We consider the y_0 such that $\frac{\partial g}{\partial y}=0$.

$$\Delta\boldsymbol{P}+2\Delta\boldsymbol{P}(\boldsymbol{\Phi}-\boldsymbol{I})(\boldsymbol{P}+y_0\Delta\boldsymbol{P})=0\tag{43}$$

By some simple matrix operation, we have

$$2(\boldsymbol{\Phi}-\boldsymbol{I})=-(\boldsymbol{P}+y_0\Delta\boldsymbol{P})^{-1}.\tag{44}$$

In (44), the $\boldsymbol{P}+y\Delta\boldsymbol{P}$ is positive semi-definite diagonal matrices, thus the $(\boldsymbol{\Phi}-\boldsymbol{I})^{-1}$ and $\boldsymbol{\Phi}-\boldsymbol{I}$ are negative semi-definite diagonal matrices when $\frac{\partial g}{\partial y}=0$. In this case, the (42) is negative semi-definite. So we can get

$$\frac{\partial g}{\partial y}=0\implies\frac{\partial^2 g}{\partial y^2}=2\Delta\boldsymbol{P}(\boldsymbol{\Phi}-\boldsymbol{I})\Delta\boldsymbol{P}\preceq 0\tag{45}$$

Thus the $g(y)=\boldsymbol{V}(\boldsymbol{p}_e+y\Delta\boldsymbol{p}_e)/R_{rr}(t)$ is quasiconcave function with respect to y and $\boldsymbol{V}(\boldsymbol{p}_e)$ is quasiconcave function with $\boldsymbol{p}_e$. Then, the constraint $\gamma\boldsymbol{I}-\sigma^2\boldsymbol{I}-\boldsymbol{A}^H\boldsymbol{V}(\boldsymbol{p}_e)\boldsymbol{A}\preceq 0$ is quasiconvex. From [11], the quasiconvex constraint can be transformed into convex constraints. Thus, the (20) is equivalent with a convex problem.

APPENDIX C
PROOF OF PROPOSITION 2

In this appendix, we provide the proof of Proposition 2. Firstly, we update the $\boldsymbol{A}^H\boldsymbol{V}(\boldsymbol{p}_e)\boldsymbol{A}$ when $P_1=\ldots=P_N$. Then we analyze the first order derivative of $\boldsymbol{A}^H\boldsymbol{V}(\boldsymbol{p}_e)\boldsymbol{A}$ to show that the $P_1=\ldots=P_N=0.5$ is the optimal solution.

When $P_1=\ldots=P_N$, we have $\mathrm{diag}(\boldsymbol{p}_e)=P_n\boldsymbol{I}$. Then the $\boldsymbol{A}^H\boldsymbol{V}(\boldsymbol{p}_e)\boldsymbol{A}$ can be written as

$$\begin{aligned}\boldsymbol{A}^H\boldsymbol{V}(P_n)\boldsymbol{A}&=\boldsymbol{A}^H[P_n\boldsymbol{I}(\boldsymbol{\Phi}-\boldsymbol{I})P_n\boldsymbol{I}+P_n\boldsymbol{I}]\boldsymbol{A}R_{rr}(t)\\&=\boldsymbol{A}^H[P_n^2(\boldsymbol{\Phi}-\boldsymbol{I})+P_n\boldsymbol{I}]\boldsymbol{A}R_{rr}(t).\end{aligned}\tag{46}$$

The derivative $\frac{\partial\boldsymbol{A}^H\boldsymbol{V}(\boldsymbol{p}_e)\boldsymbol{A}}{\partial P_n}$ is written as

$$\begin{aligned}\frac{\partial\boldsymbol{A}^H\boldsymbol{V}(\boldsymbol{p}_e)\boldsymbol{A}}{\partial P_n}&=\boldsymbol{A}^H[2P_n(\boldsymbol{\Phi}-\boldsymbol{I})+\boldsymbol{I}]\boldsymbol{A}R_{rr}(t)\\&=\boldsymbol{A}^H[2P_n(\boldsymbol{\Phi}-\boldsymbol{I}+\frac{1}{2P_n}\boldsymbol{I})]\boldsymbol{A}R_{rr}(t).\end{aligned}\tag{47}$$

When $P_n=0.5$, the $\boldsymbol{\Phi}-\boldsymbol{I}+\frac{1}{2P_n}\boldsymbol{I}=\boldsymbol{\Phi}$ is positive semi-definite matrix. When $P_n<0.5$, the $\boldsymbol{\Phi}-\boldsymbol{I}+\frac{1}{2P_n}\boldsymbol{I}$ has negative eigenvalues. When $P_n>0.5$, the $\boldsymbol{\Phi}-\boldsymbol{I}+\frac{1}{2P_n}\boldsymbol{I}$ is positive definite matrix. The $P_n=0.5$ is a minimum point of $\boldsymbol{A}^H\boldsymbol{V}(\boldsymbol{p}_e)\boldsymbol{A}$. Then, when $P_n=0.5$, the $\boldsymbol{A}^H\boldsymbol{V}(\boldsymbol{p}_e)\boldsymbol{A}$ achieves its minimum $\lambda_{\max}$.

REFERENCES

[1] L. Neng-Jing and Z. Yi-Ting, "A survey of radar ECM and ECCM," *IEEE Trans. Aerosp. Electron. Syst.*, vol. 31, no. 3, pp. 1110–1120, Jul. 1995.
[2] V. S. Chernyak, "Adaptive mainlobe jamming cancellation and target detection in multistatic radar systems," in *Proc. Int. Radar Conf.*, Beijing, China, Oct. 1996, pp. 297–300.
[3] C. J. Baker and A. L. Hume, "Netted radar sensing," *IEEE Aerosp. Electron. Syst. Mag.*, vol. 18, no. 2, pp. 3–6, Feb. 2003.
[4] K. Yeo, Y. Chung, H. Yang, J. Kim, and W. Chung, "Reduced-dimension DOD and DOA estimation through projection filtering in bistatic MIMO radar with jammer discrimination," *IET Radar, Sonar Navigat.*, vol. 11, no. 8, pp. 1228–1234, Aug. 2017.
[5] M. Ge, G. Cui, and L. Kong, "Mainlobe jamming suppression for distributed radar via joint blind source separation," *IET Radar, Sonar Navigat.*, vol. 13, no. 7, pp. 1189–1199, Jul. 2019.
[6] H. Dai, X. Wang, Y. Li, Y. Liu, and S. Xiao, "Main-lobe jamming suppression method of using spatial polarization characteristics of antennas," *IEEE Trans. Aerosp. Electron. Syst.*, vol. 48, no. 3, pp. 2167–2179, Jul. 2012.
[7] X. Wang, Y. Liu, and T. Huang, "A random antenna subset selection jamming method against multistatic radar system," in *Proc. IEEE Radar Conf. (RadarConf)*, Florence, Italy, Sep. 2020, pp. 1–6.

[8] S. L. Johnston, "Comments on 'an approximate improvement factor expression in terms of interference spectrum,'" *IEEE Trans. Aerosp. Electron. Syst.*, vol. 31, no. 2, pp. 852–854, Apr. 1995.
[9] N. Valliappan, A. Lozano, and R. W. Heath, Jr., "Antenna subset modulation for secure millimeter-wave wireless communication," *IEEE Trans. Commun.*, vol. 61, no. 8, pp. 3231–3245, Aug. 2013.
[10] J. F. White, "Matrix analysis," in *High Frequency Techniques: An Introduction to RF and Microwave Design and Computer Simulation*. Piscataway, NJ, USA: IEEE Press, 2004, pp. 161–182.
[11] S. P. Boyd, and V. Lieven, *Convex Optimization*. Cambridge, U.K.: Cambridge Univ. Press, 2004.

XIANGTUAN WANG received the B.S. degree in electronic engineering from Tsinghua University, Beijing, China, in 2015. She is currently pursuing the Ph.D. degree with the Intelligence Sensing Laboratory (ISL), Department of Electronic Engineering, Tsinghua University. Her current research interests include electronic countermeasure, joint radar-communication system design, signal processing, and optimization methods.

TIANYAO HUANG received the B.S. degree in telecommunication engineering from the Harbin Institute of Technology, Heilongjiang, China, in 2009, and the Ph.D. degree in electronics engineering from Tsinghua University, Beijing, China, in 2014.

From 2014 to 2017, he was a Radar Researcher with Aviation Industry Corporation of China (AVIC). Since July 2017, he has been with the Intelligent Sensing Laboratory (ISL), Department of Electronic Engineering, Tsinghua University, as an Assistant Professor. His current research interests include signal processing, compressed sensing, and joint radar communications system design.

YIMIN LIU (Member, IEEE) received the B.S. and Ph.D. degrees (Hons.) in electronics engineering from Tsinghua University, China, in 2004 and 2009, respectively.

In 2004, he was with the Intelligence Sensing Laboratory (ISL), Department of Electronic Engineering, Tsinghua University. He is currently an Associate Professor with Tsinghua University, where his field of activity is study on new concept radar and other microwave sensing technologies. His current research interests include radar theory, statistic signal processing, compressive sensing and their applications in radar, spectrum sensing, and intelligent transportation systems.